Fiorini Deborah

HIGH RESOLUTION HYPERSPECTRAL AND DISCRETE ANALYSIS OF ADAMELLO GLACIER ICE – CORE SECTIONS

University of Milano-Bicocca
Supervisor: Prof. Valter Maggi
Co-Supervisor: Prof. Monica Sisti
Co-Supervisor: Prof. M. C. A. Potenza

Email: d.fiorini@campus.unimib.it
Telephone number: 3406397443
Graduation date: 25 October 2022

Introduction

Ice-covered surfaces of the planet are a pristine glimpse on the climate history of the Earth. Their capability to reflect the solar radiation affects the energy budget through time, so that paleoclimatic information recorded in polar and mountain glaciers tell a story about climate and environmental changes. Climate variations are a glaring reality due to a progressive climate warming that has been observed since the 1950s. The latest 2022 IPCC report [1], highlights the worrying state of the entire cryosphere health. Mid-latitude glaciers, e.g., are highly sensitive to the current atmospheric warming, which is seriously compromising the quality of the signal preserved in the ice.

Ice core studies from mid-latitude mountain glaciers are essential to infer recent climate variability and anthropogenic impact on a regional scale. In the scientific literature, various imaging non-destructive systems have been presented to extract information from visual stratigraphy of ice cores using transmittance [2], to identify annual layers thickness and the relationships with depth in a shallow Antarctic ice core [3] and to determine annual layer thickness by linking visual stratigraphy and impurities [4]. Advanced techniques can be developed to improve the accuracy of ice cores measurements.

In this thesis, a non-destructive system based on a hyperspectral imaging sensor can be used to analyze optical properties of ice cores at the EuroCold Laboratory (University Milano-Bicocca). Hyperspectral imaging spectroscopy is a powerful technique used to characterize material’s surfaces on the basis of their optical properties. Considering that different materials and internal features vary the ice capability to absorb and reflect the electromagnetic radiation (e.g. the visible light), in this context the reflectance and derived parameters, Albedo, Snow Darkening Index (SDI) and Impurity Index (II), depending on ice properties, will be extracted and analyzed to obtain continuous records along a portion of an ice core. The SDI record will be used to select samples for discrete dust concentration analyses, in order to extract a calibrated curve for concentration variations along the entire ice core without further destructive analyses. We will consider ice-core sections extracted by the project ADA270 in 2021 from the Adamello-Mandrone glacier group region, for a length of 21 m, from 14 m to 35 m depth. The drilling site was the Pian di Neve portion of the Adamello-Presanella glaciers in the Alpi Retiniche at an altitude of 3200 m. The used drilling method is the Electrothermal Drill (ET), which uses a ring-shaped heating portion in the coring head to melt an annulus around the ice to be cored, exploiting a resistance using an electrical power, to heat the head, feed through a cable.

Material and Methods

The hyperspectral configuration considered in this work (Fig. 1) is a scanning system that consists of different parts [5]. The main mobile components are a hyperspectral imaging spectrometer (Hyperspec® VNIR, HeadWall Photonics) and a dedicated halogen stable light source (600 W, LOT Quantum Design) which can be rotated to optimize the illumination of the ice section aligning the beam in the center of the axis along sections. Both the spectrometer and the light source are able to move back and forth to scan ice core sections at a defined speed, appositely chosen to provide the right micro-step motion to obtain high spatial resolution images (up to 20 µm). The HeadWall spectrometer is a very important component of the system. It collects spectral radiance in 840 bands in VIS and NIR wavelengths (ranging from 380 to 1000 nm). Due to the low temperatures that the imaging spectrometer has to deal with (it works at about -20 °C), in the cold room two heaters keep the internal temperature at about 10 °C. Another fundamental component of the system is the white reference (a white Spectralon panel), used to reproduce an ideal reflectance equal to 1 (maximum value). The Spectralon is placed at the top of each section, on the fixed flat system's surface.

Fig. 1: Image of the hyperspectral system consisting of: a) high-precision linear stage with samples holder and motor driver; b) HeadWall camera; c) halogen lamp; d) calibrated Lambertian Spectralon® panel useful to calculate reflectance; e) PC connected to the spectrometer through a dedicated interface; f) Single-Board RIO with Ethernet TCP/IP wireless connection – Credit: Garzonio et al.

The data acquisition software was developed by R. Garzonio et al. [5]. This software allows to set the scanning parameters and synchronize the motion with the hyperspectral measurement collection for obtaining high spatial resolution images. Its graphical user interface (GUI) allows to manually define the start position (i.e., as relative position from the linear stage origin on the white panel) and the length of the scan. To have an idea regarding scanning times, to scan a 1 m ice core with a spatial resolution of 0.1 mm the system takes around 20 min. It's important to highlight that the scanned sections' surfaces are previously cut, assuming a hemicylindrical shape, to create a flat surface that the lamp can uniformly illuminate. Before measurements begin, each section is manually treated with a blade to smooth the flat surface and try to reduce possible optical artifacts. In addition, a soft brush removes the residual ice material.

The data processing software (developed in MATLAB) allows the calculation of the spectral reflectance from hyperspectral images in Digital Numbers. It is designed to handle large files (e.g. a hyperspectral image of 6000 lines, 1000 rows, and 840 bands takes up 6 GB on the hard drive) mapping them to temporary files that can be accessed as a dynamic memory, accelerating file reading and writing. From the GUI, before the processing starts, the user can select the hyperspectral image of a section, the corresponding DC file (a Dark Current image acquired before each measurement) and the output filename. Furthermore, the operator circles the white reference panel area within the image and the region of the section, before starting the analysis. The software so created extracts images where each single pixel is described by a reflectance spectrum. This information is used to construct a matrix of reflectance footprints for entire ice cores, with files that take up less memory space.

Finally, once data acquisition and processing have been performed, the results extraction can be pursued. Ice structures and light-absorbing impurities can be characterized using different spectral descriptors derived from reflectance images. The albedo, e.g., is a very important widely used property to characterize the amount of energy reflected by a surface. Regarding snow and ice, albedo is fundamental since it regulates the energy balance of glaciers and snow fields and consequent effects on climate. Furthermore, two spectral descriptors, Snow Darkening Index (SDI) and the Impurity index (II), are used to characterize the light-absorbing impurities contained in the ice. In particular, SDI is correlated with the concentration of mineral dust in snow [6] and II was originally developed to evaluate the impact of light-absorbing impurities on the albedo of the Greenland ice sheet from satellite data [7]. In this thesis, all the three spectral descriptors mentioned above are extracted from reflectance information considering indices formulas as Di Mauro et al. [6].

The record of the SDI index, as mentioned above, is also used to select samples for a concentration analysis, which requires first the decontamination of samples. The instrument for these measurements is a Coulter Counter Beckman Multisizer 4E (CC). The inserted parameters for the functioning are here reported: the control mode is Volumetric (1000 μL); the electrolyte solution is the BCI ISOTON II (a filtered, phosphate-buffered solution); the sample backer is an Accuvette ST; the sizing threshold is 1 μm; the aperture current is 800 μA; the gain of the preamplifier is a value equal to 4; the number of bins is 400, with a size bins from 1 μm to 30 μm; the bin spacing is setted as log diameter; the setted value for the sample density is 2.5 g/mL. To these analyses, 4 groups of ice features have been considered: high SDI peaks, medium-high SDI peaks, high albedo peaks and medium-high albedo peaks. These peaks are respectively associated to high impurity content, medium-high impurity content, high ice light reflection and presence of air bubbles.

Experimental results and discussion

At this point, the reflectance matrix along core sections has been created. With this file, it's possible to extract reflectance curves for each pixel band in precise regions of interest to observe optical properties when internal ice features vary. As an example, reflectance curves can be seen in Fig. 2 for a section labeled #058. The camera, as described above, measures wavelength ranging from 380 nm to 1000 nm.

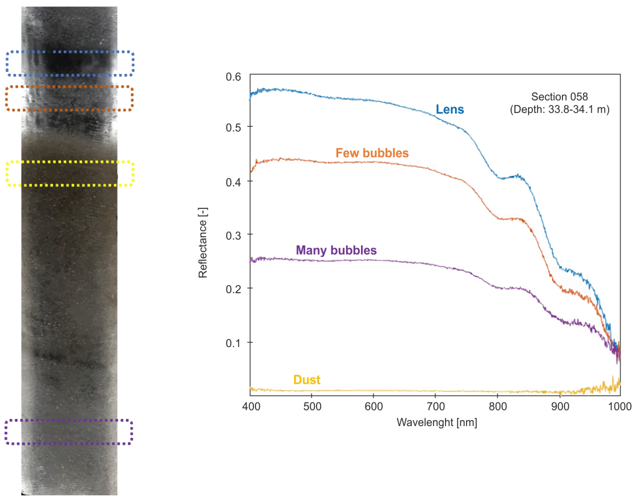

Fig. 2: reflectance curves for a 0.3 m long ice-core section analyzed, labeled #058. Different ice features vary the optical properties moving along the selected section.

As expected, impurities strongly decrease the reflectance and ice lenses rapidly increase it. Bubbles have a particular behavior, halfway between dust and lenses. The section considered here is of particular interest due to the high concentration of impurity contained, as will be seen from CC measurements. Moving the HeadWall camera step-by-step from the top to the bottom of each section, all the records for Albedo, SDI and II are created from these curves. One index record, SDI trend, can be seen in Fig. 3. There are many high peaks, in particular three of them are of greatest interest: the peak between 23-24 m, the one between 25-26 m and the last one between 33.5-34 m. This last is the one that corresponds to the section labeled #058 in Fig. 2.

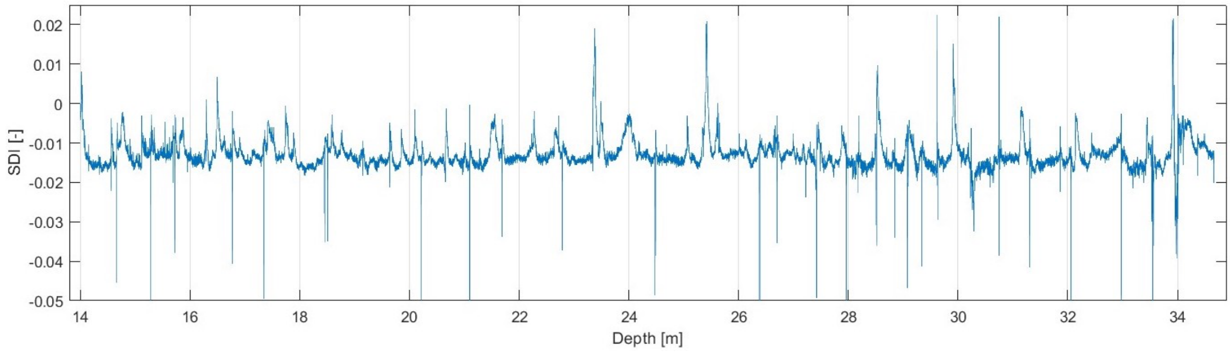

Fig. 3: continuous record for the Snow Darkening Index (SDI), along all the scanned sections

Specifically, for high impurity concentration samples, exactly the peaks mentioned above have been used. Due to the high SDI, samples have been diluted prior to the analysis. The overall results showed a particles concentration in the order of $(12.93 \pm 3.67)\ ppm$ for high SDI samples. Samples from ice lenses highlighted a low particles concentration in the order of $(0.58 \pm 0.40)\ ppm$. Samples with medium SDI values displayed particles concentrations in the order of $(5.91 \pm 3.21)\ ppm$ and samples with visible air bubbles generally had low concentrations, in the order of $(0.19 \pm 0.09)\ ppm$. After the use of a regression model, the calibrated curve is obtained (Fig. 4).

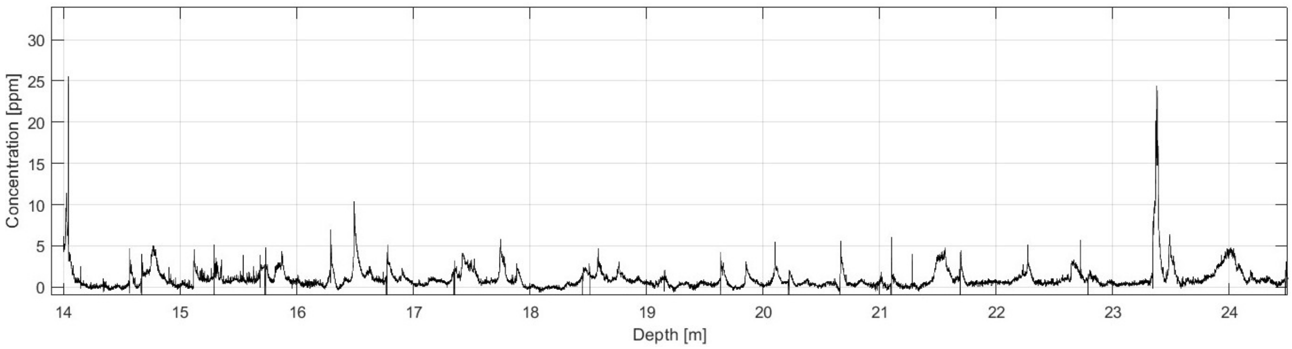

Fig. 4: portion of the calibrated curve for concentration along the analyzed ice-core sections

The calibration curve so extracted highlights forecast regions with low, medium or high impurity concentration. The concentration variation ranges from 0 ppm to a maximum of about 30 ppm. In this graph portion, there is one very high peak and some medium peaks. The average trend ranges between just over 0 ppm and just under 5 ppm. As can be seen from graphs, when the illumination from the lamp reaches the ice smoothed surface, different effects must be taken into consideration. The incident electromagnetic radiation e.g. penetrates for a few millimeters within the surface creating multiple scattering emissions, which could generate reflectance artifacts such as abrupt indices variations. The analysis made during this thesis showed promising results that can be further investigated to map ice-core properties related to the past. The integration of hyperspectral imaging analyses with classic ice core measurements will allow a comprehensive view of chemical and physical properties of ice cores all over the world.

References

[1] https://www.ipcc.ch/report/ar6/wg2/downloads/report/IPCC_AR6_WGII_SummaryVolume.pdf
[2] https://agupubs.onlinelibrary.wiley.com/doi/full/10.1029/2008JD011083
[3] https://citeseerx.ist.psu.edu/document?repid=rep1&type=pdf&doi=12cd158fe2999bced407463b292332add20fafa8
[4] https://epic.awi.de/id/eprint/12321/1/Sve2005a.pdf
[5] https://www.sciencedirect.com/science/article/abs/pii/S0165232X17305797
[6] https://agupubs.onlinelibrary.wiley.com/doi/full/10.1002/2015JD023287
[7] https://ui.adsabs.harvard.edu/abs/2014NatGe...7..509D/abstract